International Journal of Material Forming (2022) 15: 28
https://doi.org/10.1007/s12289-022-01660-0

ORIGINAL RESEARCH

A dynamic data driven application system for real-time simulation of resin transfer moulding processes

Gorka Garate[1] · Isabel Harismendy[2] · Oihane Echeverria-Altuna[2] · Julián Estévez[1]

Received: 26 November 2021 / Accepted: 21 January 2022 / Published online: 31 March 2022

Abstract
This paper presents a numerical solution to optimize RTM processes based on a DDDAS methodology, taking permeability as stochastic. The model proposed in this investigation allows real-time accurate prediction of the filling rate by adjusting the parameters with the on-line captured process data. The suitability of the proposed model was tested and validated under different process parameters variations like pressure and preform permeability.

Keywords DDDAS · Resin transfer moulding · Darcy · Permeability

Introduction

Due to the intrinsic complexity of Resin Transfer Moulding (RTM) processes, simulation is a very useful tool for the design of the part and for the optimization of the process conditions of the composites manufactured. Usually virtual physics-based models solved by FEM are used, but their main drawback is the long calculation time, which makes them useless for online predictive systems. In addition, these models use a static combination of parameters that represents the behavior of the real system. In this case, the disadvantage lies at the variability of the parameters of the design phase in the real-time process. As the values of those parameters are not static but stochastic, the outputs of these simulated models often present significant deviations from those of the corresponding real processes [1, 2].

In the RTM process preform porosity and permeability and resin viscosity are required as input parameters for the physical models used to simulate mould filling [3]. However, parameters such as permeability and porosity cannot be estimated accurately beforehand as a consequence of preform architecture variability due to different handling and storage conditions or shear deformations during the forming/draping stage, nesting effects during lay-up, low resistance channels along the preform, as well as accidental misplacement of the preform in the mould [3]. Several experimental and simulation studies have outlined the stochastic nature of permeability. Standard deviations up to 20% were observed during permeability measurements [4–8], while according to other results permeability standard deviation can reach values up to 30%, as in [9].

To circumvent this stochastic nature of permeability (and other parameters) DDDAS (Dynamic Data Driven Application Systems) methods can be applied. It was Dr. Darema who coined the DDDAS paradigm [10]: "DDDAS entail the ability to incorporate additional data into an executing application. These data can be archival or collected on-line; and in reverse, the ability of applications to dynamically steer the measurement process". In all cases, the common feature is that the simulation can process online field data from measures and adapt to those measurements.

DDDAS systems have been mostly applied in Computational Science and Engineering and Mathematics, and also been some research in the field of Environmental Sciences [11] or Materials Science [12]. However, only a few examples can be found for composite materials [13, 14]). These examples address only mechanical properties and not manufacturing processes, excepting the work of Chinesta et al [15], where Hybrid Twins Features of which DDDAS systems are a constitutive part were illustrated for RTM. In this case the RTM process was performed in a radial injection with a isotropic reinforcement and the flow front was measured visually.

✉ Gorka Garate
gorka.garate@ehu.eus

[1] Faculty of Engineering, University of the Basque Country UPV/EHU, Donostia, Spain

[2] Industry and Mobility Unit, Tecnalia (Member of Basque research & Technology Alliance), Donostia-San Sebastian, 20009, Spain

Following this line of work, this paper presents a Dynamic Data Driven Application System for a lateral injection of a anisotropic reinforcement for the real time adjustment of parameters based on pressure sensors data. The method presented in this work allows to operate in real time during a 2D RTM process, detecting the discrepancies between the virtual simulation and the data from the running RTM experiment and correcting them on the fly. More specially, the model proposed allows to optimize filling rate in a RTM process by adjusting the parameters to the experimental measures of the actual filling rate taken in real time, taking into account the noises in both the predictions and the measured data.

The suitability of the proposed model was tested using four different preform configurations and process conditions.

This paper is divided in six sections.

Section "Proposed virtual offline model" details the proposed mathematical model used for the theoretical simulations of the virtual model and "Proposed model for the DDDAS RTM simulation" details the proposed DDDAS model.

Section "Experimental" describes the materials, setup and execution of the four test RTM experiments used in this paper.

Section "Results and discussion" presents the results obtained by the DDDAS model for the four RTM experiments of the previous section, showing its adaptability to the different configurations.

Finally, "Conclusions" presents the conclusions and future lines of work.

Proposed virtual offline model

The method of simulation consists in solving by finite differences the following 2D Initial Value Problem (IVP):

$$\begin{cases} \boldsymbol{v}(\boldsymbol{x},t) = \dfrac{d\boldsymbol{x}}{dt} = -\dfrac{\boldsymbol{k}(\boldsymbol{x})}{\mu}\nabla p(\boldsymbol{x},t) & \text{(1a)} \\ \boldsymbol{x}(0) = \boldsymbol{g} & \text{(1b)} \end{cases}$$

This IVP consists of Darcy's law for the filtration velocity of the flow in the i direction, plus a condition for the initial position of the front of the flow. In Eq. 1a $\boldsymbol{v}$ is the Filling rate, $\boldsymbol{k}$ is the permeability tensor of order 2, μ is the viscosity (scalar), p is the pressure, $\boldsymbol{x}$ is the vector pointing to the front of the flow and $\boldsymbol{g}$ is the initial gap between the edge of the preform and the contour line. The IVP is defined in domain Ω (see Fig. 1). The boundary of the domain consists of the pressure contour, the impermeable boundary and the goal line.

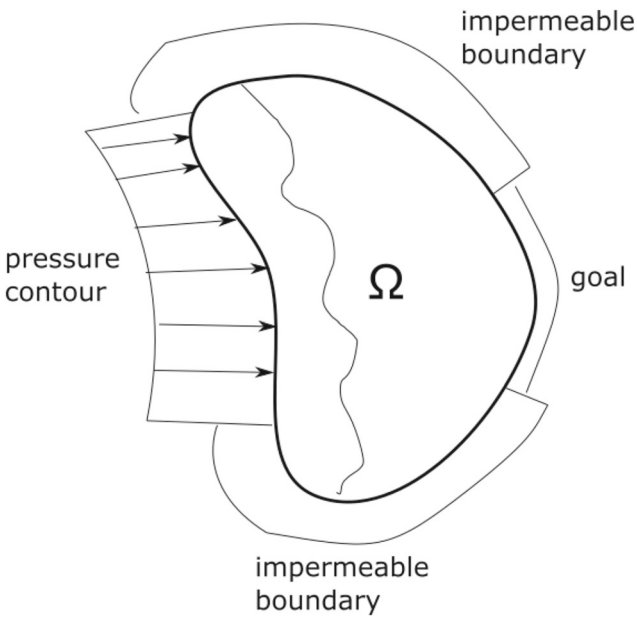

Fig. 1 Domain

In two- or three-dimensional RTM settings permeability is sometimes modelled as a second- or third-order tensor in order to take into account the anisotropy of the configuration, but here the permeability $\boldsymbol{k}(\boldsymbol{x})$ is taken a scalar function. Nevertheless, the methodology here developed can easily be generalized to the 2D tensor case.

The two-dimensional forward model for RTM is purely rheologic and does not include thermal and chemical phenomena. Thermal phenomena are neglected because the temperature during the experiments simulated has been proven to remain practically constant; the evolution of viscosity during the curing stage is left for future work. In the case of the experiments here presented the viscosity of the resin remained constant at the selected temperature through the injection stage (Fig. 2).

Approximating the differentials by finite increments and assuming through each step a constant pressure gradient and a constant permeability tensor, we can iterate on the position of the front of the flow and generate simulations of the RTM processes for different variations of the parameters. The pseudo-code of the generation of the theoretical simulations is presented here as Algorithm 1.

Proposed model for the DDDAS RTM simulation

Figure 3 describes the way the DDDAS works. The model starts with an initial state of the RTM process. An initial discrete front of one hundred points located along the width of the mould at an initial separation from the injection line ($x = x_0$ mm). Another two hundred points are fixed at the

impermeable boundary (in the case of our mould, $y = 0$ mm and $y = 125$ mm) and one hundred more are fixed at the goal line ($x = 530$ mm). The nominal value of permeability is set to an initial value.

Algorithm 1 Generation of the RTM simulations.

Initialization : $n = 0$; $\boldsymbol{x}^0 = \boldsymbol{g}$; $t^0 = 0$;
while *all points at the goal line have not been reached* **do**
  Time step: $t^{n+1} = t^n + \Delta t$;
  for *every point at the front of the flow* **do**
    Calculate the pressure gradient ∇p^n at the point of the front of the flow;
    Approximate the filling rate at step n using Eq. 1;

$$\boldsymbol{v} = \frac{d\boldsymbol{x}}{dt} = -\frac{\boldsymbol{k}}{\mu}\nabla p^n \tag{2}$$

    Approximate the advance in position of the front at point $\boldsymbol{x}^n$ at step n;

$$\boldsymbol{a}^n = \Delta t \cdot v_i^n \tag{3}$$

    if *the advance* $\boldsymbol{a}^n$ *has crossed the impermeable boundary* **then**
      Apply a non-penetration condition

$$\boldsymbol{a}^n = \boldsymbol{a}_{in}^n + \left(\boldsymbol{a}_{out}^n - \left(\boldsymbol{a}_{out}^n \cdot \boldsymbol{n}\right)\boldsymbol{n}\right), \tag{4}$$

      where $\boldsymbol{n}$ stands for the normal vector at the impermeable vector (see Fig. 2);
    end
    if *the goal line has been crossed* **then**
      Apply a no-penetration condition using Eq. 4;
    end
    Approximate the position of the front at point $\boldsymbol{x}^{n+1}$ at step $n + 1$;

$$x_i^{n+1} = x_i^n + \boldsymbol{a}^n \tag{5}$$

  end
  if *all points on the goal line have been reached* **then**
    break;
  end
end

The simulation proceeds using Algorithm 1, assigning at each of the points in the actual front (at each iteration step) a stochastic value of the permeability obtained from a normal Gaussian distribution that uses as mean the nominal value of the actual permeability of the simulation and a fixed standard deviation of 2.5% of the nominal permeability.

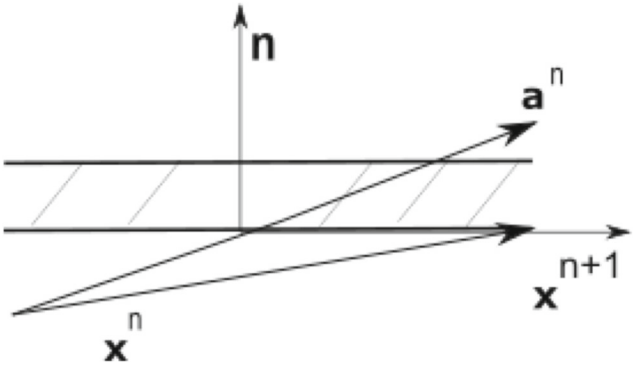

Fig. 2 Impermeable boundary

The predicted state given by the model provides the following outputs (these magnitudes are user-defined):

1. Predicted average position of all the points in the front (along x coordinate in mm)
2. Predicted average filling rate of all the points in the front (along x coordinate in mm/s)

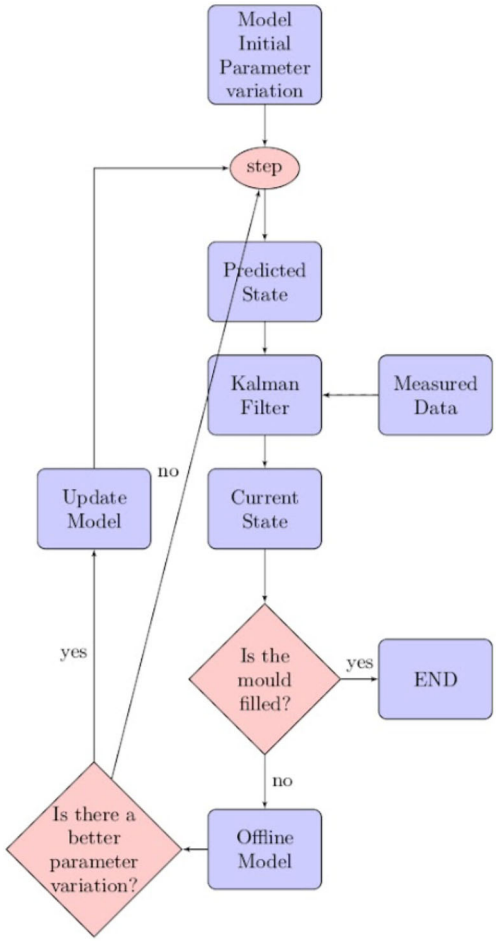

Fig. 3 DDDAS flow chart

3. Predicted pressure of a sensor at point (0.15,0.0575) (in Pa)

The model uses both the estimate and the measured value to apply a Kalman filter that gives a new filtered current filling rate estimate.

If the mould is not filled, the model checks whether there is a precalculated variation (permeability value) for the actual front position that gives a filling rate that is closer to the estimate than that of the actual variation. If there is one, the model updates the permeability value taking the corresponding value of the offline model that performs best.

The process goes on taking new steps using the new parameter until it finds new data (in that case the Filter + Current State + Update is repeated) or the mould has been filled (the points in the front have reached the goal line). The pseudo-code is detailed in Algorithm 2.

Algorithm 2 Generation of the DDDAS RTM simulation.

```
Initialization : n = 0; pick up values x^0 and parameter
k^0 from a previously simulated variation; t^0 = 0 ;
while all points at the goal line have not been reached
do
    Time step: t^{n+1} = t^n + Δt;
    Take a single step to time t^{n+1} using Algorithm 1;
    if there is collected data recorded for the current
    front position t^{n+1} then
        Step 1 of the Kalman filter: Measure;
        Step 2 of the Kalman filter: Update;
        Step 3 of the Kalman filter: Estimate:
        • Look among the recorded simulations the variation that
          best approximates the estimated filling rate for the
          given front position;
        • Update parameter k to the new simulation;
    end
    if all points on the goal line have been reached then
        break;
    end
end
```

As regards the Kalman filter, the values of the errors used have been:

- Data error in position of the front and in filing rate: 15%
- Initial estimate error: 25%
- Process error: 25%

The outputs of the DDDAS RTM simulation for each step are (these magnitudes are user-defined):

1. Corrected permeability (in m^2)
2. Average position of all the points in the front (along x coordinate in mm)
3. Average filling rate of all the points in the front (along x coordinate in mm/s)
4. Virtual pressure at point (0.15,0.0575) (in Pa)

Experimental

An unidirectional glass fiber supplied by Saertex (Ultra Fatigue UD) was selected for the RTM experiments. Fibre properties are summarized in Table 1:

Preforming was performed under in a vacuum table at 150ºC for 90 seconds.

In order to check the suitability of the proposed model for detection and correction of the parameters, different kind of preforms were prepared with the following configurations (Fig. 4):

- Configuration 1: preforms with constant permeability (4 layers of glass fabric).
- Configuration 2: preforms with different permeability zones. For this purpose, the number of plies was reduced from 4 to 3 and 0 in a specific area of the preform as shown in Fig. 4.

To take into account the possible interaction of the resins and the binder, a commercial low viscosity epoxy supplied by Resoltech (1800/1805) was used as the infiltration fluid. This resin has a constant viscosity of 25 cps at all the temperature/times of the experiments.

Unidirectional laminar flow RTM tests were carried out at a constant pressure in a rectangular mould with transparent glass cover. Both a camera and a pressure sensor were used to monitor the progress of flow front in the mould.

The main features of the equipment are shown in Fig. 5.

The RTM injection test were performed at 60ºC and pressures gradient ranging from 0.5 bar to 2 bar. The geometry considered is a rectangular mould cavity of 530 mm in length, 115 mm in width and of thickness 3.9 mm. A pressure sensor form Kistler (Type 4001A, with temperature compensation) is located 155 mm from the inlet (Figs. 6 and 7).

A computerized data acquisition system is used to assemble the experiments data (temperature, pressure, camera recordings) and calculate online the flow front position from the camera and pressure sensors readings.

Flow front position front the pressure sensors was calculated from measured pressure gradient, assuming that pressure decreases linearly from $P_0(t)$ at point x_0 to 0 on the flow front at a distance $xs(t)$ from x_0.

$$\frac{dP}{dx} = -\frac{P_0(t)}{x_s(t)} \tag{1}$$

Table 1 Fibre properties

Weaving pattern	E-glass unidirectional non-crimp fabric (NCF)
Areal weight	1176 ± 64 g/m^2
Powder	Huntsman XB 6078 10 ± 2 g/m^2
Sewing thread	Polyester 76 dtex 12 ± 3 g/m^2

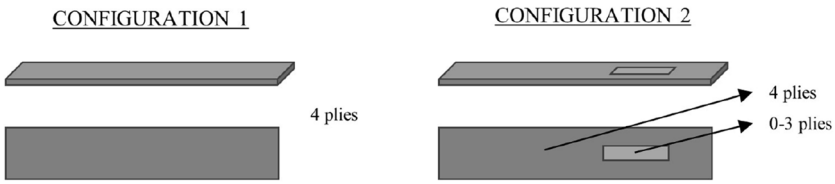

Fig. 4 Preforms configuration

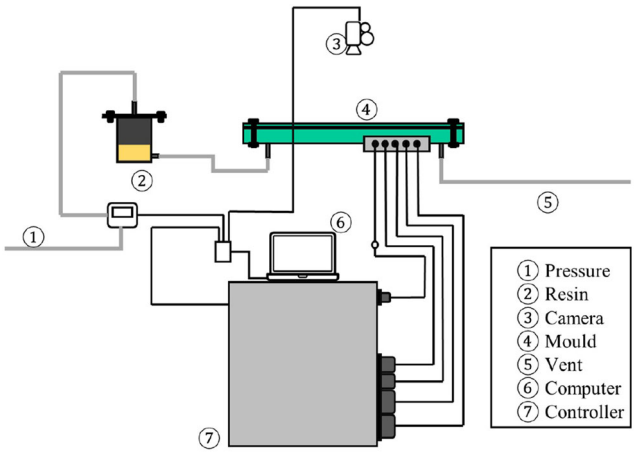

Fig. 5 Schematic diagram of the test equipment

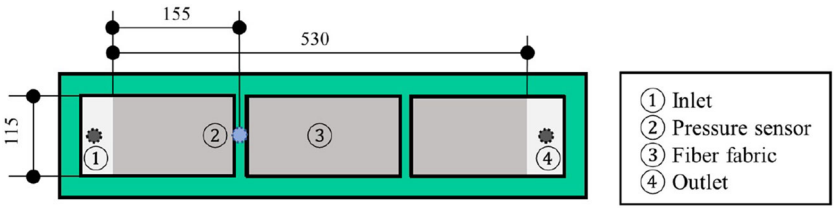

Fig. 6 RTM mould

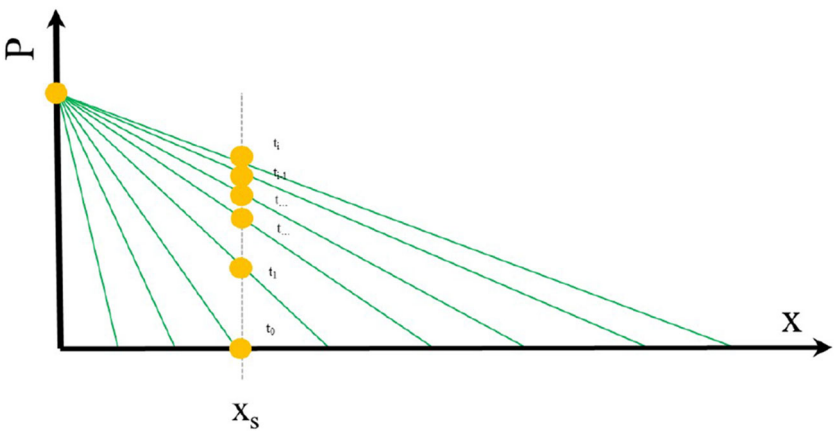

Fig. 7 Pressure evolution with time at sensor location *xs*

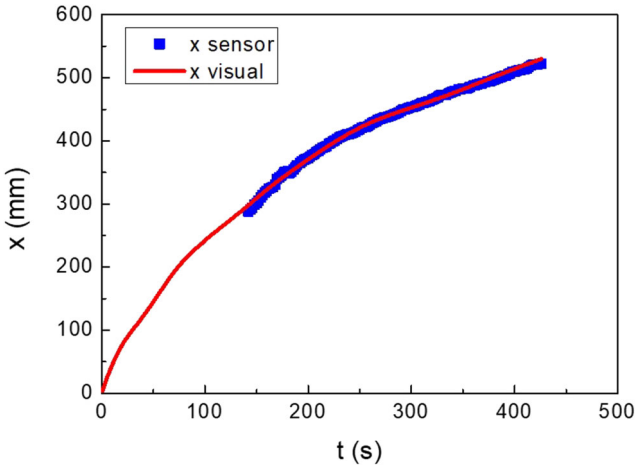

Fig. 8 Comparison between the flow front position calculated by camera and based on pressure sensor

Figure 8 shows, as an example, the comparison between the flow front position calculations from the camera and pressure sensor readings. As it can be seen, there is a good correlation between both methods.

The monitoring strategy presented, with a single pressure sensor is only valid for a unidirectional flow experiment. However, pressure sensing can be used to reproduce the flow front shape in more complex geometries.

For instance, Fratta et al [16]. coupled pressure signals and flow modeling in an algorithm to estimate flow front patterns in 2D geometries using few sensors placed in strategic positions. The developed method is based on the partition of the cavity shape into a combination of flow channels Each flow channel contains a flow path and follows its development through the cavity from the inlet to the outlet, as. The algorithm for flow front

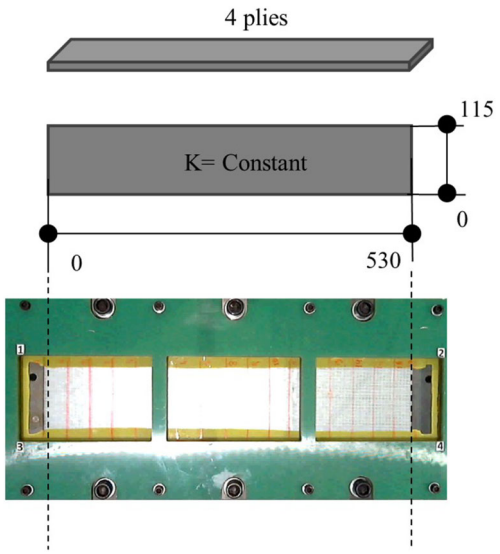

Fig. 9 Test 1 configuration

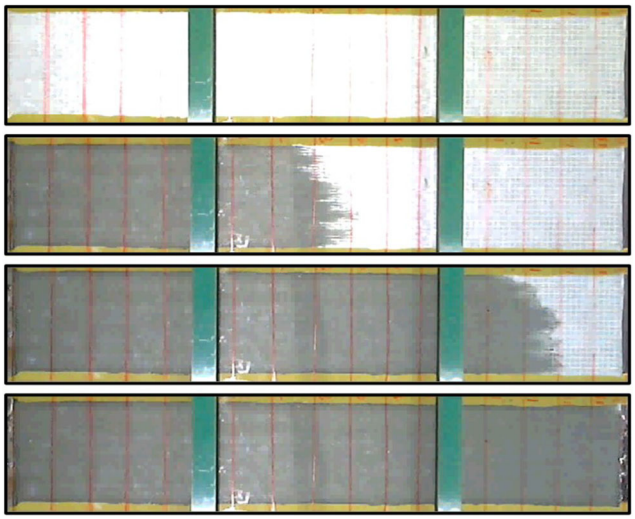

Fig. 10 Flow front progression during Test 1

estimation is thus applied to each channel separately, approximating the whole 2D injection by a combination of concurrent injections along the defined flow paths into the

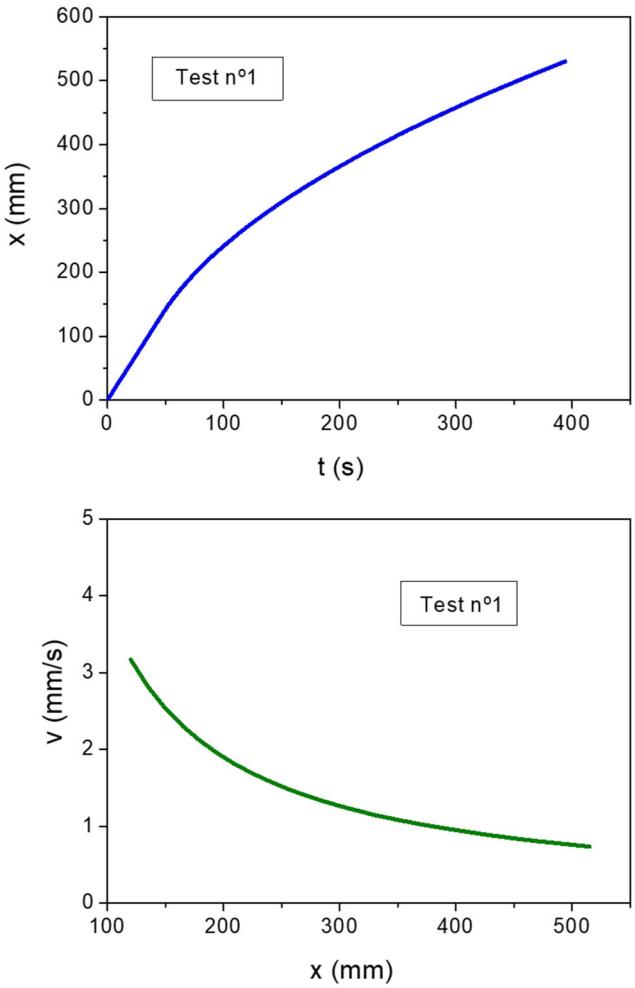

Fig. 11 Experimental results for Test 1. Flow front position and filling rate

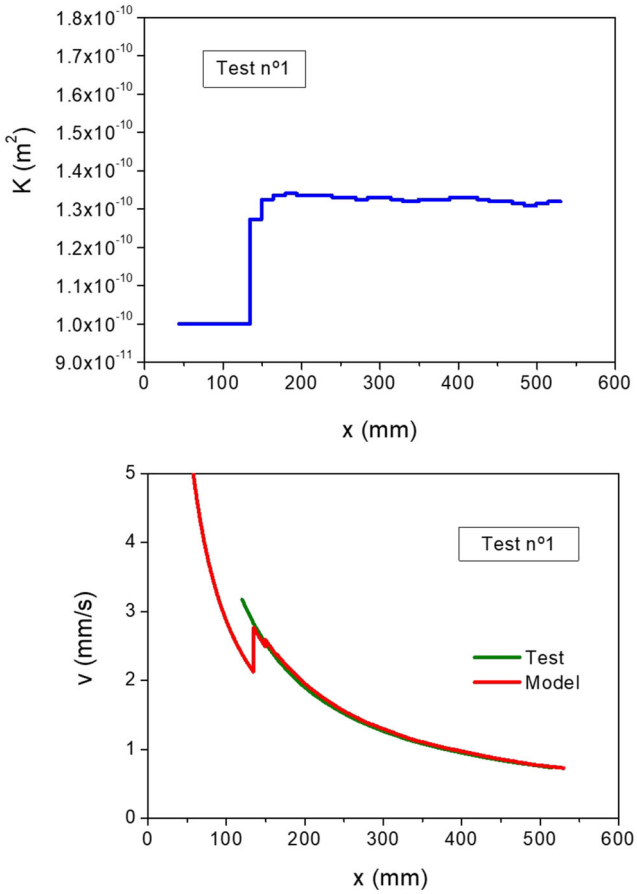

Fig. 12 Model results for Test 1. Flow front position and filling rate

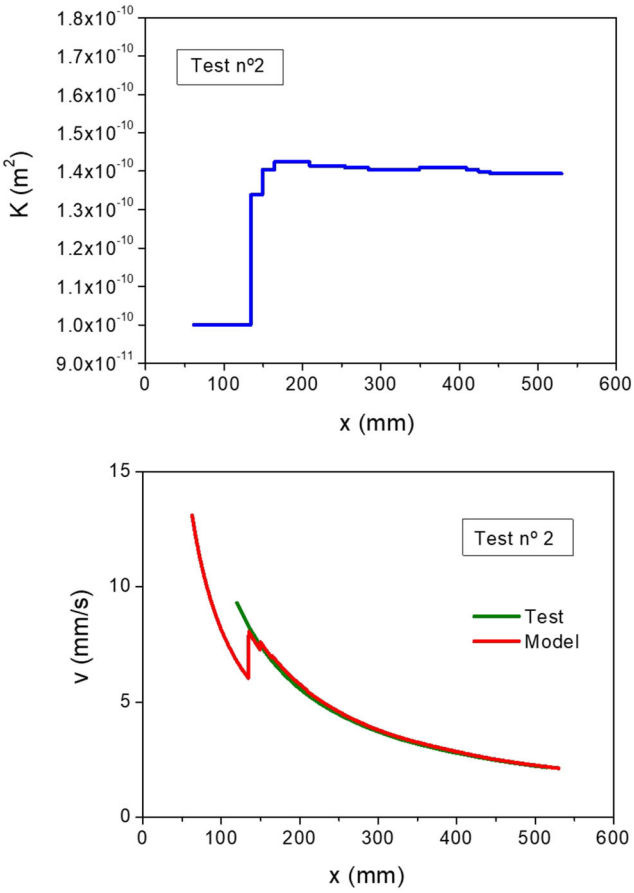

Fig. 14 Model results for Test 2. Flow front position and filling rate

corresponding channels. The complete flow front profile at a given impregnation time is finally reconstructed by interpolating the determined flow front positions along the flow paths.

For complex 3D geometries the number of sensors and locations will depend of the race tracking regions and strength, the inlet and vent locations and the mold geometry, which is translated by the superimposed pressured

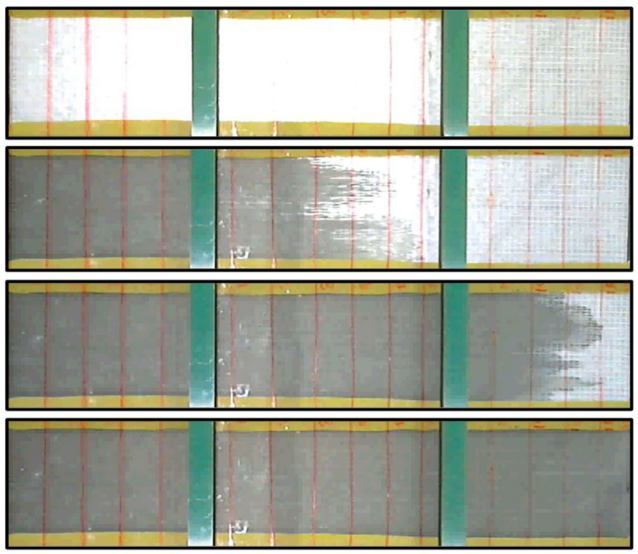

Fig. 13 Flow front progression during Test 2

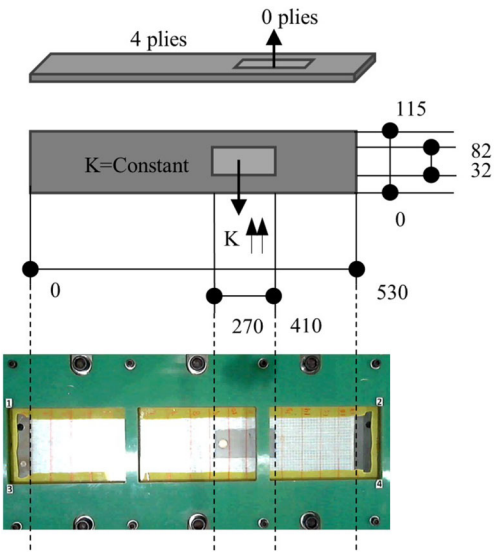

Fig. 15 Test 3 configuration

gradients maps. For this purpose, a simplified cost-effective simulation-based methodology has been proposed by Siddig et al. [17]. This methodology extrapolates sensors locations for a rectangular geometry to more complex shapes.

Results and discussion

The suitability of the proposed model was tested using four different preform configurations and process conditions, called hereafter Tests 1 to 4.

Test 1

Figure 9 shows Test 1 configuration. It was performed with a constant permeability preform consisting of 4 plies of the glass fabric, with a resultant fibre volume content Vf of 47.5% and a nominal permeability of $1.35e^{-10}$ m^2. The test was carried out under controlled vacuum. at −0.73 bar.

As can be seen in Fig. 10, the flow front was stable, with no racetraking and little difference between the saturated (full preform impregnated, dark grey) and unsaturated (preform partially impregnated, lighter grey) areas. The saw-tooth aspect of the flow front is due to the presence of high permeability channels between fibre tows.

Figure 11 shows the actual flow front position and filling rate evolution during Test 1.

Figure 12 shows the results of the on-line model calculations for Test 1. An onset permeability of $1.0e^{-10}$ m^2 was used in order to check the online adaptation ability of the DDDAS model. As can be seen in the figure, permeability value was quickly recalculated to the nominal permeability as soon as the model received the real data from the experiment, showing a good fitting between the filling rate values calculated by the model and the experimental values.

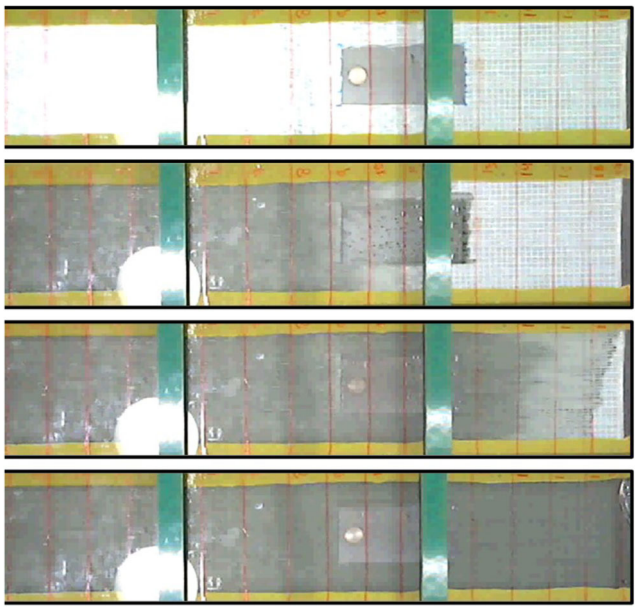

Fig. 16 Flow front progression during Test 3

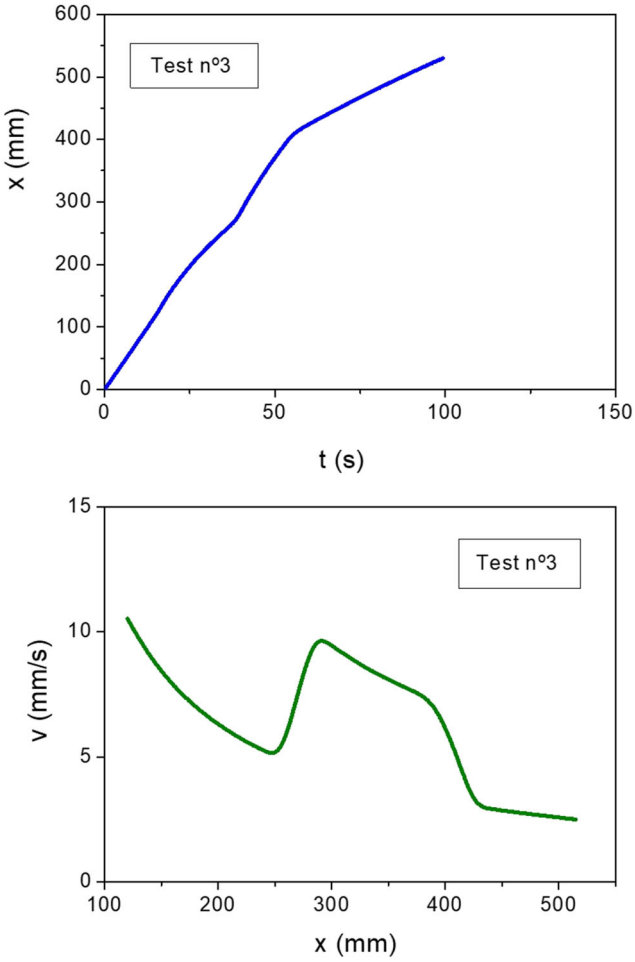

Fig. 17 Experimental results for Test 3. Flow front position and filling rate

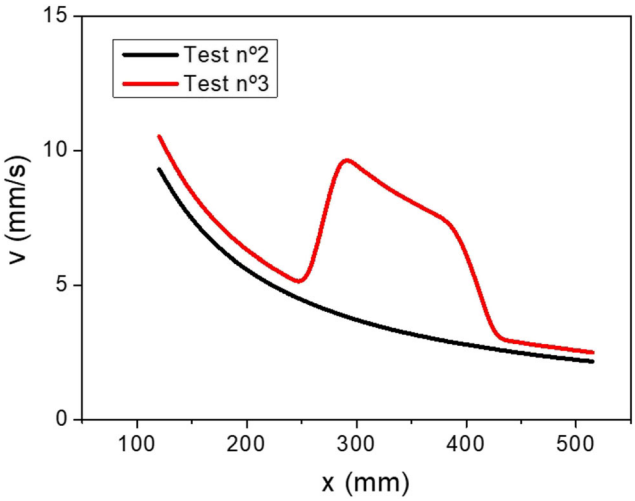

Fig. 18 Filling rate vs flow front position for Test 2 and Test 3

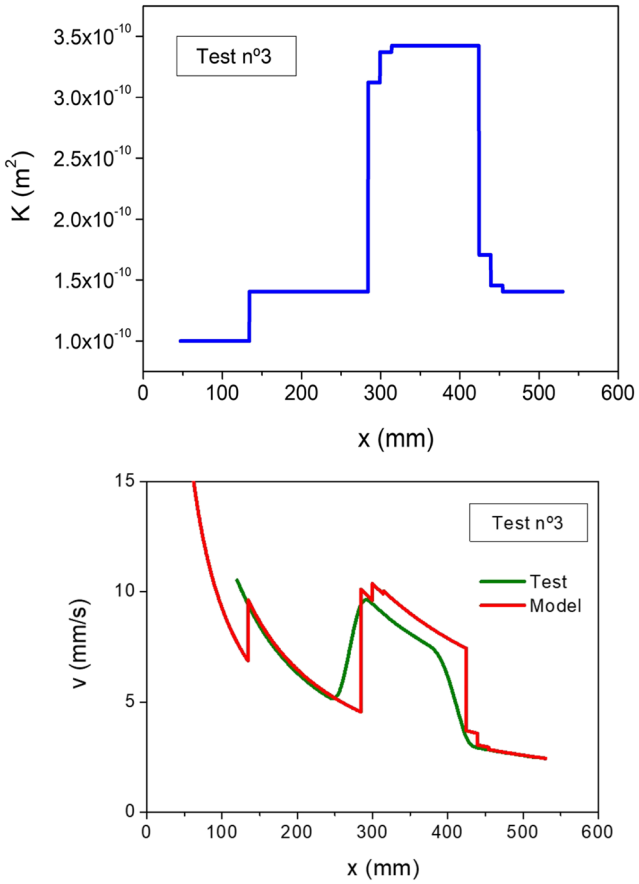

Fig. 19 Model results for Test 3. Flow front position and filling rate

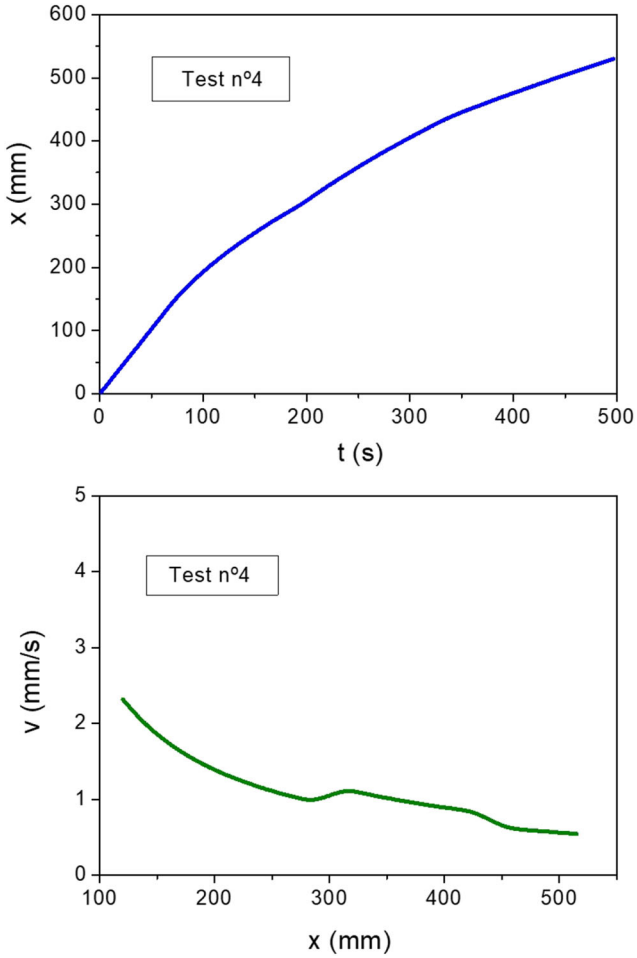

Fig. 21 Experimental results for Test 4. Flow front position and filling rate

Test 2

Test 2 was performed with the same preform configuration as Test 1: a constant permeability preform, with a nominal

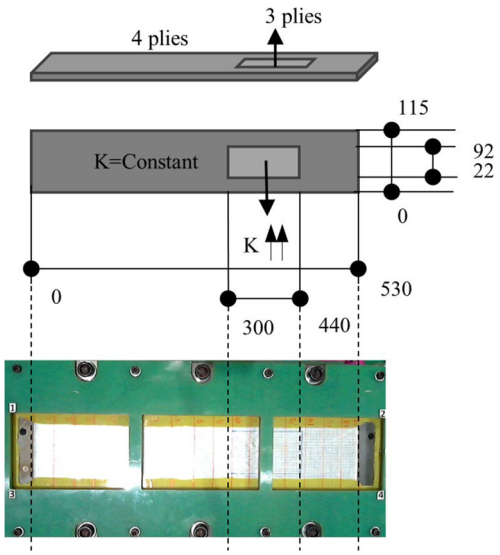

Fig. 20 Test 4 configuration

permeability value of $1.35e^{-10}$ m^2 (Fig. 9). The difference between both tests was the pressure gradient applied. In this case the test was performed under vacuum (−0.98. bar) and a constant injection pressure of 1.04 bar, resulting in a pressure gradient of 2.02 bar.

The increase of the filling rate intensifies the effect of the high permeability channels and significantly increases the difference between the saturated and the unsaturated flow.

Figure 13 shows the saturated flow front evolution.

Figure 14 shows the results of the on-line model calculations for Test 2. Again, an onset permeability of $1.0e^{-10}$ m^2 was used. As can be seen in the figure, permeability value was quickly adapted to real data even at high filling rates.

Test 3

Test 3 was performed with a variable permeability preform. For this purpose, the number of plies was reduced from 4 to 0 in a specific area of the preform. The test was carried out under vacuum (−0.98 bar) and at a constant

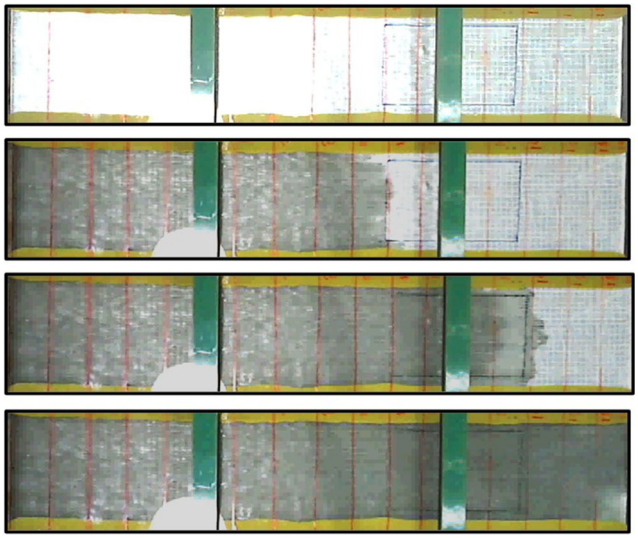

Fig. 22 Flow front progression during Test 4

injection pressure of 1.32 bar (pressure gradient of 2.30 bars) (Figs. 15 and 16).

As for Test 2, there was a significant difference between the saturated and the unsaturated flow rates. The filling rate dramatically increased in the high permeability window producing a turbulent flow with bubbles (Fig. 16).

In this case, the different permeability zones were clearly appreciated in Fig. 17 by the change of the flow front vs time and filing rate vs flow front position curves shapes.

Figure 18 compares the results obtained for Tests 2 and 3. As can be seen, the filling rates were similar in the 4 plies zones and then sharply increased for test 3 in the high permeability window. Filling rate is slightly higher for test number 3 due to a higher pressure gradient (2.3 vs 2.02 bar).

As shown in Fig. 19, the model was able to detect an adapt to abrupt permeability changes giving a good prediction of filling rate.

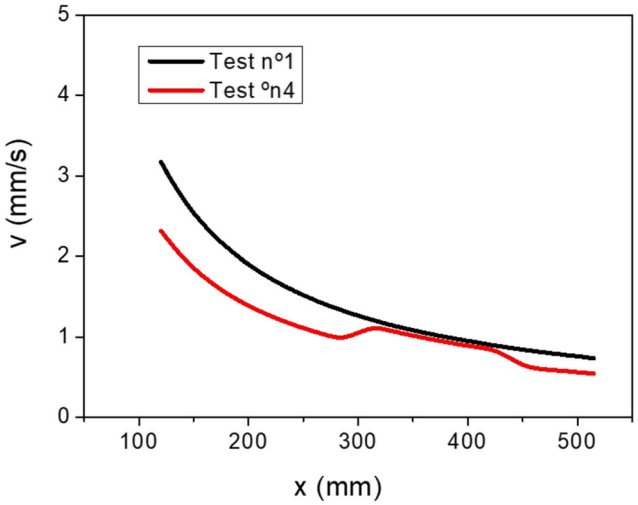

Fig. 23 Filling rate vs flow front position for Test 1 and Test 4

Test 4

Figure 20 shows Test 4 configuration. As in Test 3, it was performed with a variable permeability preform. In this case, the number of plies was reduced from 4 to 3 in a specific area of the preform, in a fiber volume variation from 47.5% to 35.6% in order to test the model at less extreme conditions. Also, the test was carried out at lower filling rate, under a constant vacuum of 0.53 bar and no injection pressure applied.

As expected, in this case the change of the filling rate was significantly less pronounced. (Figures 21) However, as seen in the figure bellow (Fig. 19), it could be clearly appreciated visually by a more unsaturated flow condition (light gray)(Figure 22).

Figure 23 compares the results obtained for Tests 1 and 4. As can be seen, the filling rates were similar in the 4 plies zones and then increased for Test 4 in the high permeability window. Again, there is a slight difference of filling rates due to the different pressure gradient applied (0.73 bar for Test 1 vs 0.53 bar for Test 4).

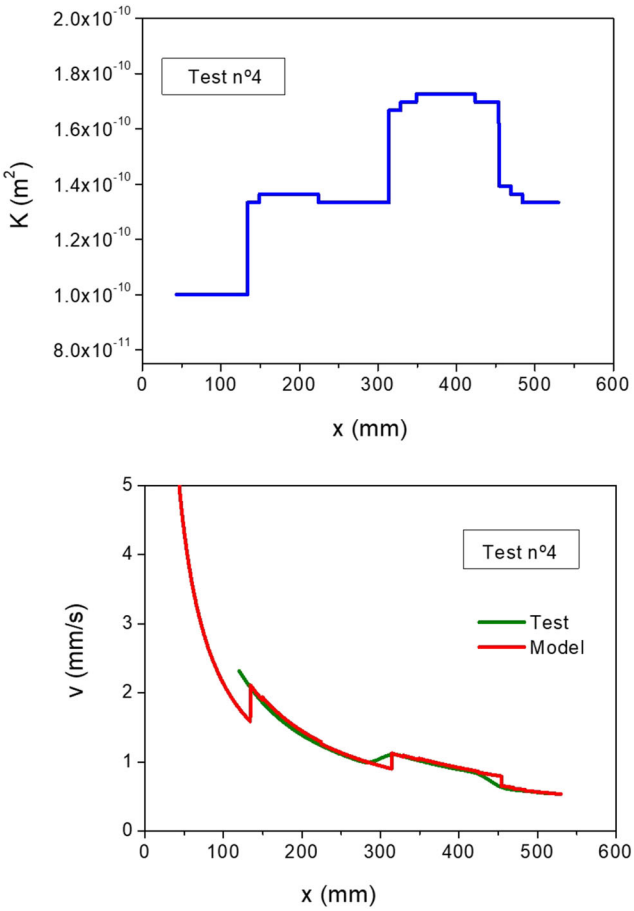

Fig. 24 Model results for Test 4. Flow front position and filling rate

Figure 24 shows the model results for Test 4. Again, the model was able to detect and recalculate permeability changes. Even if the differences are less pronounced, the model gives an accurate prediction of the filling rate.

Conclusions

The proposed DDDAS model was able to calculate in real time the filling rate under different process conditions. The model was able to detect and adapt to both abrupt and smooth permeability changes in the experiments, giving accurate predictions. The developed solution allows the online estimation of the evolution of the filling process and its uncertainty. This estimation can be utilized to carry out control and corrective actions during manufacturing, potentially increasing process efficiency, improving part quality and reducing process failures and defects.

In this work temperature and viscosity remained constant at the experiment's conditions and its variability was not taken into account for the model. Future work will include viscosity variations through thermal and chemical phenomena.

Acknowledgements The authors wish to thank University of the Basque Country UPV/EHU for the Open Access funding provided for the publication of this paper.

Funding Open Access funding provided thanks to the CRUE-CSIC agreement with Springer Nature. This work has been partially supported by Ministerio de Ciencia e Innovación project PID2020-116346GB-I00.

Declarations

Conflict of Interests The authors declare that they have no conflict of interest.

References

1. Tifkitsis A, Skordos A (2018) Integration of stochastic process simulation and real time process monitoring of lcm sampe. Conference 18, Southampton, UK
2. Zhang F, Cosson B, Comas-Cardona S, Binetruy C (2011) Efficient stochastic simulation approach for rtm process with random fibrous permeability. Compos. Sci. Technol., 71, https://doi.org/10.1016/j.compscitech.2011.06.006
3. Mesogitis TS, Skordos AA, Long AC (2020) Uncertainty in the manufacturing of fibrous thermosetting composites: a review. Archives of Computational Methods in Engineering 27:105–134. https://doi.org/10.1016/j.compositesa.2013.11.004
4. Desplentere F, Woerdeman DL, Lomov SV, Verpoest I, Wevers M, Bogdanovich A (2005) Micro-ct characterization of variability in 3d textile architecture. ComposSci Technol, 65(13)
5. Dinescu D, Hoes K, Sol H, Parnas RS, Lomov S (2004) Study of nesting induced scatter of permeability values in layered reinforcement fabrics. Composites Part A 35(12):1407–18
6. Luthy T, Hintermann M, Mosler H, Ziegmann G, Ermanni P (1998) Dependence of the 1-d permeability of fibrous media on the fiber volume content: comparison between measurement and simulation. Struct Mater 3:433–42
7. Verleye B, Lomov SV, Long A, Verpoest I, Roose D (2010) Permeability prediction for the meso?macro coupling in the simulation of the impregnation stage of resin transfer moulding. Composites Part A 41(1):29–35
8. Potter K, Khan B, Wisnom M, Bell T, Stevens J (2008) Variability, fibre waviness and misalignment in the determination of the properties of composite materials and structures. Composites Part A 39(9):1343–54
9. Endruweit A, McGregor P, Long AC, Johnson MS (2006) Influence of the fabric architecture on the variations in experimentally determined in-plan permeability values. Compos Sci Technol 66(11-12):1778–92
10. Darema F (2004) Dynamic data driven applications systems: A new paradigm for application simulations and measurements. 4th International Conference on Computational Science (ICCS 2004); Lecture Notes in Artificial Intelligence 3038:662–669. https://doi.org/10.1007/s11831-018-9301-4
11. Ouyang Y, Zhang JE, Luo SM (2007) Dynamic data driven application system: Recent development and future perspective. Ecol Model 204:1–8. https://doi.org/10.1016/j.ecolmodel.2006.12.010
12. Ghnatios C, Masson F, Leygue A, Cueto E, Chinesta F (2012) Proper generalized decomposition based dynamic data-driven control of thermal processes. Comput Methods Appl Mech Eng 213-216:29–41. https://doi.org/10.1016/j.cma.2011.11.018
13. Prudencio E, Bauman PT, Williams SV, Faghihi D, Ravi-Chandar K, Oden JT (2013) A dynamic data driven application system for real-time monitoring of stochastic damage. International Conference on Computational Science, ICCS 2013 18:2056–2065. https://doi.org/10.1016/j.procs.2013.05.375
14. Paton Pozo PJ (2016) Dynamic data driven applications systems (dddas) for multidisciplinary optimisation (mdo). Master's Thesis, Cranfield University
15. Chinesta F, Cueto E, Abisset-Chavanne E, Duval JL, El Khaldi F (2020) Virtual, digital and hybrid twins: A new paradigm in data-based engineering and engineered data. Archives of Computational Methods in Engineering 27:105–134. https://doi.org/10.1007/s11831-018-9301-4
16. Fratta CD, Koutsoukis G, Klunker F et al (2016) Fast method to monitor the flow front and control injection parameters in resin transfer molding using pressure sensors. Compos. Materials 50:2941–2957. https://doi.org/10.1177/0021998315614994
17. Siddig N, Binetruy C, Syerko E, Simacek P, Advani S (2018) A new methodology for race-tracking detection and criticality in resin transfer molding (rtm) process using pressure sensors. J Compos Mater 52(29):4087–4103. https://doi.org/10.1177/0021998318774829